PHILOSOPHICAL TRANSACTIONS A

royalsocietypublishing.org/journal/rsta

Research

Cite this article: Woods AW, Stock MJ. 2019 Some fluid mechanical constraints on crystallization and recharge within sills. *Phil. Trans. R. Soc. A* **377**: 20180007. http://dx.doi.org/10.1098/rsta.2018.0007

Accepted: 14 November 2018

One contribution of 15 to a Theo Murphy meeting issue 'Magma reservoir architecture and dynamics'.

Subject Areas:
volcanology, fluid mechanics, geophysics

Keywords:
stratified cumulate layers

Author for correspondence:
Andrew W. Woods
e-mail: aww1@cam.ac.uk

Downloaded from https://royalsocietypublishing.org/ on 04 March 2022

Some fluid mechanical constraints on crystallization and recharge within sills

Andrew W. Woods[1] and Michael J. Stock[2]

[1]BP Institute for Multiphase Flow, University of Cambridge, England CB3 OEZ, UK
[2]Department of Earth Sciences, University of Cambridge, England CB2 3EQ, UK

The injection of hot magma into a sill can lead to heating and melting of the walls and roof of the reservoir while the injected magma cools and crystallizes. If the crystals are relatively dense, they will try to sediment from the injected magma to form a cumulate layer. In this cumulate layer, the crystals form a porous framework which traps the melt as it is built up. As the melt within the sill continually cools and precipitates dense crystals, there will be a gradual reduction in the density of the remaining silicate liquid. As a result, the melt which is progressively trapped in the pore space of the cumulate layer will become stably stratified in density. Using an idealized model of the fluid mechanical and thermodynamical principles, we explore some of the controls on the thickness and density stratification of cumulate layers following replenishment of a sill-like magma chamber. We show the balance between jamming of the crystal laden melt to form a homogeneous layer and the formation of a stratified cumulate zone depends on the cooling time scale compared to the sedimentation time scale. A key finding is that the composition and stratification in a packed crystal–melt suspension and the associated cumulate layer formed by cooling an intrusion of hot melt injected into the crust may have considerable variability, depending on the properties of the overlying roof melt and the size and hence fall speed of crystals which form in the melt.

This article is part of the Theo Murphy meeting issue 'Magma reservoir architecture and dynamics'.

1. Introduction

There has been considerable interest in the structure of the crust in regions of active volcanism (e.g. [1–4]). Recent

THE ROYAL SOCIETY PUBLISHING

© 2019 The Author(s) Published by the Royal Society. All rights reserved.

Downloaded from https://royalsocietypublishing.org/ on 04 March 2022

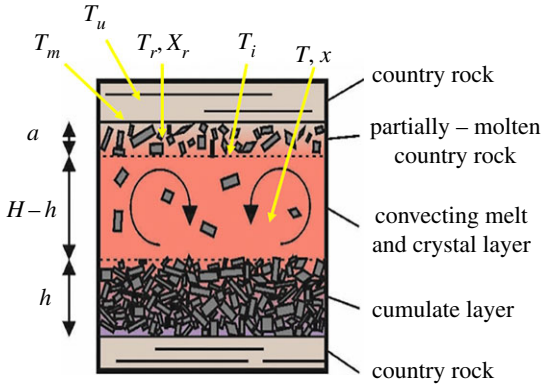

Figure 1. Idealized model of a cooling and convecting melt-rich sill, which forms a cumulate layer at the base by crystal settling, while melting the roof. Some of the crystals released from the partially melted roof layer may sediment into the underlying melt, leading to a hybrid composition of the melt–crystal basal cumulate.

petrological, geochemical and geophysical constraints point to a picture in which magmatic systems transcend the entire crust and comprise a vertical distribution of sills, containing magmas of different compositions and crystallinities [5–9]. In general, the magma becomes progressively more fractionated with height in the crust, as new melts injected into deeper sills cool and crystallize high melting point minerals; these minerals may form cumulate mush layers, while some of the remaining silicate liquid ascends to shallower crustal levels [10,11].

If the melt intrudes a pre-existing sill, the dynamics of the intrusion depend on the density and viscosity contrast with the existing magma in the sill, and also the density and mechanical properties of any crystal-rich cumulate layers in the sill [12,13]. If the new magma is hotter and denser than the melt, but less dense than bulk density of the cumulate layer, it will tend to intrude below the existing melt and above the cumulate layer (figure 1). This can lead to heat transfer between the two layers of magma and between the new magma and the cumulate layer. As the new magma cools, it forms crystals which may settle from the melt, while the original melt and the cumulate layer will be heated up, resorbing some of their crystals and becoming progressively more mobile. Since the density of the melt evolves with temperature and crystal content, as the magmas and cumulate layer gradually equilibrate thermally, the density of the different regions may evolve leading to some intermingling or mixing of the magmas, such as characterized by mafic inclusions or hybrid magmatic compositions [12,14–16].

The evolution of the magma is complex and depends in part on the crystal content of the melt and the properties of the cumulate layer in the sill. In turn, these depend on the earlier thermal evolution of the system. Although one can envisage a wide range of possible scenarios, it is of interest to explore an idealized physical model to provide some constraints on the evolution of the chamber, and provide insight into some of the processes. This approach forms the basis of the present paper. To set the scene, we first explore an idealized situation in which we follow the evolution of a body of melt cooling from above as it crystallizes and develops a cumulate layer. In particular, we follow the evolution of the magma crystal content, the density of the melt and the associated evolution of the basal cumulate layer. A key new result is the recognition that the cumulate layer may become stably stratified in density, and we explore the controls on this process. We then examine the implications of this stratification and how the crystal content of existing magmas within sills can impact the thermal evolution of the melt. The presence of stratification can have a significant impact in suppressing the mixing and interaction of the cumulate with the new melt.

The structure of the paper is as follows: in §2, we present some model calculations of the density and crystal content of an idealized melt with temperature for (i) a general Icelandic

Downloaded from https://royalsocietypublishing.org/ on 04 March 2022

composition and (ii) a composition similar to the melt at Soufriere Hills Volcano, Montserrat. We then present an idealized model for the thermal evolution of an intrusion of melt, in order to gain some insight into the controls on the partitioning of crystals between the cumulate layer and the crystals in suspension. We illustrate how this model may be used to calculate the density stratification of the cumulate layer. In §4, we discuss the possible impact of such stratification on the intrusion and cooling of a new body of hot melt injected into the sill from deeper in the crust. In §5, we present some preliminary analogue experiments, which begin to identify the dynamics of more complex systems in which melts are intruded into high-crystallinity mushes in or close to a jammed state. Finally, in §6, we draw some conclusions and discuss the geological importance of these findings.

2. Density evolution of crystallizing melt

As magmas cool in the crust, a series of minerals crystallize sequentially, depending on the composition of the primary melt and intrinsic conditions within the system (i.e. pressure, oxygen fugacity). Controls on the order and abundance of precipitating minerals are complex, but have been experimentally well-constrained for a range of melt compositions and pressures (e.g. [17–20]). This has allowed development of thermodynamic models for predicting magmatic crystallization sequences as a function of temperature (e.g. [21,22]) and general principles can be drawn, especially in the context of following the density of the mixture (e.g. [23,24]). Some of the most abundant crystals that precipitate from terrestrial silicate melts include: olivine with densities greater than 3200–3300 $\mathrm{kg\,m^{-3}}$, and plagioclase with a density of approximately 2600 $\mathrm{kg\,m^{-3}}$ [25]. If the net density of the crystals precipitating from a melt is greater than the melt density, then the melt density will decrease, while if it is smaller, the melt density will increase during crystallization, depending also on the composition and depth in the crust. As cooling and as crystallization proceeds, there may also be a change in the dominant mineral which precipitates.

In figure 2*a*, we show the crystal content and density of a typical enriched Icelandic melt as a function of temperature [30], while in figure 2*b* we show an analogous figure for a melt which fed Soufriere Hills volcano, Montserrat [26].

In the Montserrat case, the crystals are dense relative to the melt, and the crystals may fall through the melt, accumulating on the floor of the chamber to form a cumulate layer. As this happens, the density of the residual melt decreases and as a result, the density of the melt trapped in the pore space between the crystals will also gradually decrease (figure 2*b*). This leads to a decrease in the melt density for crystal fractions less than about 70%, and will lead to a decrease in the bulk density of the cumulate layer with time as the trapped melt becomes progressively less dense.

In the Iceland case, the melt is much denser, and the plagioclase crystals which precipitate are in fact less dense than the melt. As a result, the melt density actually increases with crystallization once the crystal fraction exceeds about 10% and plagioclase comes on to the liquidus. The occurrence of an Icelandic melt density minimum at the onset of plagioclase crystallization was identified recently by Hartley & Maclennan [33]. The production of less dense crystals leads to the possibility of a roof cumulate as well as at the floor of the intrusion. If the density of the melt gradually decreases, then the melt trapped in the roof cumulate will be stably stratified while the melt in the floor cumulate will become unstably stratified. In the next section, we develop a model for the cooling and crystallization to explore some of the controls on the formation of cumulate layers.

3. A model for cumulate formation

As a simplified model of the formation of a cumulate layer, we draw from the work of Huppert & Sparks [13] who modelled the cooling and crystallization of a melt subject to cooling from above with the assumption that the melt remains well-mixed. We combine this with a model for the

Downloaded from https://royalsocietypublishing.org/ on 04 March 2022

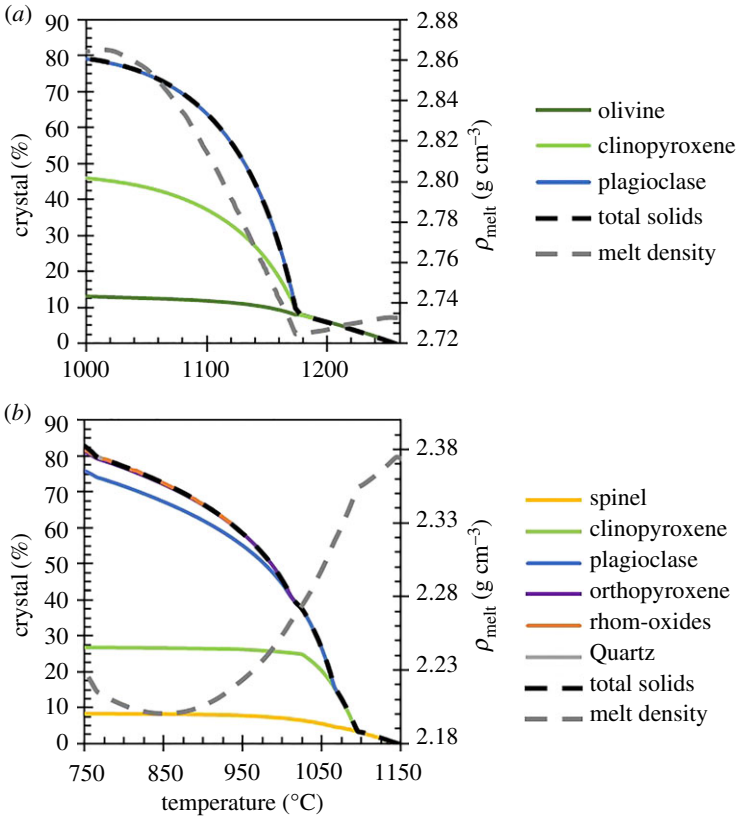

Figure 2. Examples of melt density and crystal content as a function of temperature for a typical enriched Icelandic melt (*a*) and a primitive melt from Soufriere Hills volcano, Montserrat (*b*). The model in (*a*) was produced using Rhyolite-MELTS [22], with the primitive whole-rock composition of nodule M27 [26] as a starting composition, 6 wt% initial H_2O, a pressure of 1.5 kbar, and an oxygen fugacity at QFM+2, (similar to [27,28]). The predicted mineralogy is not identical to that in Montserrat erupted products (i.e. amphibole is absent, likely with concurrent overstabilization orthopyroxene). This likely reflects an inherent limitation of the model to accurately predict hydrous mineral stabilities [22,29] but is not expected to significantly impact the predicted density evolution. The model in (*b*) was produced using the Petrolog software [21], with a calculated enriched Icelandic primary melt as the starting composition [30], 0.15 wt% initial H_2O, a pressure of 4 kbar and an oxygen fugacity of QFM-1 [31,32]. In the Icelandic case, the melt density initially decreases but then increases as plagioclase begins to precipitate, while for Montserrat, the density falls as relatively dense crystals form from a relatively low-density melt phase.

sedimentation of crystals through the melt which leads to the formation of a cumulate layer [34]. The model accounts for the evolution of the magma density as the magma crystallizes and the cumulate layer builds up, trapping progressively more and more evolved melt as the crystals sediment and leading to a heterogeneous deposit. The model also accounts for the cooling and crystallization of the convecting magma, and illustrates conditions under which the crystal content may increase sufficiently to lead to jamming and formation of an immobile mush zone above the cumulate.

(a) Evolution of the new magma

The evolution of the injected magma, initially of depth H, may be described by equations for the evolution of the temperature, T, and crystal content, x, of the melt and the depth of the cumulate layer, h. We can then follow the evolution of the density of the melt ρ as crystals form. For simplicity, we initially assume that there is one dominant phase which crystallizes, and that

Downloaded from https://royalsocietypublishing.org/ on 04 March 2022

the crystals are dense relative to the melt. While the layer of melt remains well-mixed, the depth of the cumulate layer h increases as crystals sediment from suspension with fall speed v_s leading to the relation

$$(1-\phi-x)\,\mathrm{d}h/\mathrm{d}t = v_s x, \tag{3.1}$$

where ϕ is the melt fraction in the cumulate, which for simplicity we assume to have value 0.4 throughout this work. We also assume that the melt layer has depth $(H-h)$ and crystal content x. The crystal content of the melt layer evolves according to the relation

$$(H-h)\,\mathrm{d}x/\mathrm{d}t = -v_s x + \beta(H-h)\,\mathrm{d}T/\mathrm{d}t + x_r v_{sr}, \tag{3.2}$$

where β is the rate of crystal production per unit degree of cooling. The first term on the right-hand side denotes the settling of crystals from the melt (cf. [16,34]). The second term represents the rate of crystal production with cooling, with $\beta = \mathrm{d}x/\mathrm{d}T$. β is nearly constant over a large range of temperature as the total crystal content increases towards values of about 0.5–0.6 (cf. figure 2) and so for simplicity we take this to be a constant herein with value $1/200\,\mathrm{C}^{-1}$. The final term in equation (3.2) represents the sedimentation of crystals from any overlying layer of partially melted and remobilized roof material associated with the heat flux into the roof of the chamber from the melt. Here, x_r is the crystal content of this remobilized roof layer and v_{sr} is the fall speed of crystals in this layer.

The thermal budget of the new intrusion of melt is given by the balance between cooling and crystallization in the melt layer, the heat flux associated with the crystals settling from the roof melt layer and the heat flux supplied to the boundaries of the chamber

$$(H-h)(\rho C_p + \rho L\beta)\mathrm{d}T/\mathrm{d}t - x_r v_{sr}\rho C_p(T_u - T) = -F, \tag{3.3}$$

for a shallow sill-like feature, the heat flux across the upper and lower boundaries will dominate. If the density gradient in the cumulate layer at the base of the melt is stable and no convection develops, then the cooling of the cumulate layer only occurs by conduction. The cumulate layer will therefore remain hot for a considerable time. The heat transfer between this layer and the main melt will then be small compared with the convective cooling at the top of the chamber. We therefore neglect the convective heat transfer at the floor for the heat balance of the melt. We return to this assumption once we have some model predictions, and thereby establish that the model results are self-consistent.

In equation (3.3), L denotes the latent heat of crystallization taken to be $3\times10^5\,\mathrm{J\,kg^{-1}}$, while the specific heat, C_p, has representative value $10^3\,\mathrm{J\,kg^{-1}\,K^{-1}}$ [13]. Finally, in equation (3.3), the second term on the left-hand side denotes the thermal energy supplied to the main body of melt associated with any crystals which may sediment from the overlying partially molten roof layer into the melt.

(b) Interface heat flux

In order to model the evolution of the system, and hence compare the sedimentation of crystals with the cooling and crystal production rate in the new magma, we require a parametrization of the heat flux across the interface. In order to establish some of the main controls on the evolution of the system, we assume the main body of melt is in a state of turbulent convection which applies provided it has a high Rayleigh number, $\mathrm{Ra} > 10^7$, where

$$\mathrm{Ra} = \frac{g\Delta\rho(\Delta T)H^3}{\kappa\mu}. \tag{3.4}$$

Here $\Delta\rho(\Delta\mathrm{T})$ is the density contrast in the melt associated with the change in temperature from the cold upper interface to the interior of the melt layer, ΔT, and κ and μ are the diffusivity and viscosity of the melt. We note that this change in density of the melt includes the effect of crystal production in the cooling melt, at the rate $\mathrm{d}x/\mathrm{d}T$, which typically dominates the change in density compared with the cooling contraction of the melt. Indeed, motivated by figure 2, we

Downloaded from https://royalsocietypublishing.org/ on 04 March 2022

assume that the density of the liquid phase in the melt ρ_m varies with temperature and hence total crystal content according to the relation

$$\frac{\mathrm{d}\rho_m}{\mathrm{d}T} = -\lambda, \tag{3.5}$$

where λ has approximate value 1.1 for Soufriere Hills-type melt and value -0.5 for Iceland-type melt. In the former case, this leads to a reduction in the melt density of about 6% as the melt crystal content increases to a mass fraction of about 0.6. The heat flux is given by (cf. [35])

$$F = 0.1\left[\frac{g\Delta\rho(\Delta T)}{\kappa\mu}\right]^{1/3}\rho C_p\kappa\Delta T. \tag{3.6}$$

The model is idealized in that it assumes the change in temperature across the boundary layer is sufficiently small that all the fluid participates in the convection: in practice, if there is a sufficient temperature drop across the interface that the melt viscosity at the interface is much higher than in the main melt, then a stagnant layer may develop [36]. However, in the present modelling, we envisage that in an active volcanic zone with many injections of melt over time, the roof layer is derived from an earlier intrusion, and so is of comparable composition to the intruded melt. Thus, we assume the melting range of the roof material is similar to but somewhat cooler than the new intrusion. In this case, we neglect the effects of any stagnant boundary zone and assume that all the melt participates in the convection in each layer.

The heat transfer law (3.6) depends on the interfacial temperature and hence the overlying material. If this is composed of a solidified crystalline melt layer from an earlier intrusion, then it will heat up this layer. Typically, once a sufficient fraction of the lowest melting temperature interstitial melt in this overlying layer changes phase, the material will be remobilized and a melt–crystal suspension will form. If this remobilized layer is less dense than the new intrusion of melt, it will remain as a separate layer, but as it is heated by the hot intrusion, it may become sufficiently mobile that after an initial transient, it will begin to convect.

In this idealized picture, the interface temperature will be given by matching the heat flux supplied from the intruded melt to the heat flux taken up by the reheated and remobilized overlying layer (cf. [13]). If the interface has temperature T_i and the remobilized layer has temperature T_r, then the interface temperature is given by the relation

$$\left[\frac{g\Delta\rho(\mathrm{T}-T_i)}{\kappa\mu}\right]^{1/3}\rho C_p(T-T_i)\kappa = \left[\frac{g\Delta\rho_r(T_i-T_r)}{\kappa_r\mu_r}\right]^{1/3}\rho_r C_p(T_i-T_r)\kappa_r, \tag{3.7}$$

where subscript r refers to the remobilized overlying layer and $\Delta\rho(\Delta T)$ denotes the change in bulk density associated with the change in temperature ΔT, accounting for the change in the melt density and also the presence of any crystals formed as a result of the change in temperature. The viscosity of the remobilized melt is likely to be larger than that of the new intrusion as it is cooler, more evolved and has a higher crystal content. We account for the increase in viscosity in the melt layer as the crystal content x increases towards a critical value at which the suspension locks, x_c, using the parametrization [37].

$$\mu = \mu_o\left(1-\frac{x}{x_c}\right)^{-5/2}, \tag{3.8}$$

where x_c is the critical crystal content for the melt–crystal mix to jam, here taken to be 0.6, and for simplicity we assume this relation applies in both the intrusion and also the zone of molten roof material.

(c) Evolution of the partially molten roof layer

The heat flux supplied to the remobilized roof layer in the chamber can lead to an increase in the temperature of this layer and also can lead to remobilization of more of the roof material by ablation of the top of the layer. If the original temperature of the solid roof material was T_u, and the temperature at which this layer becomes remobilized is T_m ($>T_u$), then, assuming a large

Downloaded from https://royalsocietypublishing.org/ on 04 March 2022

Rayleigh number in this layer, the convective heat flux from the remobilized layer of temperature T_r into the overlying static roof material is given by the approximate relation

$$F_u = 0.1\left[\frac{g\Delta\rho_r(T_r - T_m)}{\kappa_r\mu_r}\right]^{1/3}\rho_r C_p(\mathrm{T}_r - T_m)\kappa_r. \tag{3.9}$$

The thermal budget of the remobilized layer, of depth $a(t)$, then takes the form

$$a(t)(\rho_r C_p + \rho_r L\beta_r)\,\mathrm{d}T_r/\mathrm{d}t = F - F_u, \tag{3.10}$$

where β_r is the rate of crystal production per unit of cooling of the roof layer, while the upper boundary of this remobilized layer grows in time at the rate $\mathrm{d}b/\mathrm{d}t$ given by

$$(\rho_r C_p(T_r - T_u) + \rho_r L\Delta x_r(T_r - T_u))\,\mathrm{d}b/\mathrm{d}t = F_u. \tag{3.11}$$

This balances the heat flux supplied to the material above the layer of roof melt, F_u, to the fraction $\Delta x_r(T_r - T_u)$ of the solid which melts as the roof is heated to temperature T_r provided that T_r is in excess of the temperature T_m required for the roof material to become mobile.

As the remobilized layer develops, some of the crystals may sediment across the interface and into the new intrusion of magma below, as discussed above, leading to a compositional evolution of the newly intruded magma. This effect will lead to an evolution of the thickness of the remobilized layer according to the relation

$$\frac{\mathrm{d}a}{\mathrm{d}t} = \frac{\mathrm{d}b}{\mathrm{d}t} - x_r v_{sr}, \tag{3.12}$$

where v_{sr} is the fall speed of the crystals in the roof melt layer, and x_r is the concentration of the crystals in the roof melt layer. In turn, the depth of the region containing the intruded magma, H, will increase through the crystal settling from the upper layer, according to

$$\mathrm{d}H/\mathrm{d}t = x_r v_{sr}. \tag{3.13}$$

We note however that if the roof melt is of higher viscosity than the newly injected magma, the crystal settling from the roof melt may be relatively slow unless there are some large pre-existing crystals in the country rock.

Finally, we note that the concentration of crystals in the remobilized layer, x_r, evolves according to the conservation relation

$$\frac{\mathrm{d}(ax_r)}{\mathrm{d}t} = (1 - \Delta x)\,\mathrm{d}b/\mathrm{d}t - x_r v_{sr} + a\beta_r \mathrm{d}T_r/\mathrm{d}t, \tag{3.14}$$

where the first term on the right-hand side is associated with the supply of the fraction $(1 - \Delta x(T_r - T_u))$ of the solid roof material in the form of crystals to the remobilized layer. This fraction depends on the temperature of the remobilized layer, T_r, but is less than $(1 - \Delta x(T_m - T_u))$, corresponding to the crystal fraction when the roof material is heated to temperature T_m and just becomes mobile. The second term accounts for the loss of crystals by sedimentation, with speed v_{sr}, from the roof melt and into the underlying intrusion of magma (§3a), and the final term denotes the change in crystal content of the roof melt associated with cooling or heating of this layer (cf. equation (3.10)).

(d) Cumulate layer density

As the cumulate layer grows, melt is trapped in the interstices between the crystals. We assume that the density of the melt evolves as crystals form in the suspension, according to the simplified relation equation (3.5). Combining this with the equation for the growth of the cumulate layer, we can predict the compositional stratification in the cumulate layer.

Downloaded from https://royalsocietypublishing.org/ on 04 March 2022

(e) Model predictions

By solving the above system of equations using a simple finite difference method with MATLAB, with a sufficiently small time step to ensure convergence of the solution, we can gain insight into the evolution of the system following the injection of a new volume of magma. We assume that over a short time, the melting of the roof material leads to a sufficiently deep layer of roof melt to drive convection (cf. [13]), and we then follow the cooling and crystallization of the melt and formation of the cumulate layer as the system evolves. In particular, we explore the density stratification in the cumulate layer which depends on the evolution of the melt and the rate of accumulation of cumulate. Although there are a range of initial conditions possible, in order to illustrate some of the key effects, we assume the roof of the chamber is initially sufficiently cold to be immobile, while the new intrusion of magma is just about to commence crystallization. We then explore how the new intrusion cools and crystallizes, while the roof material is reheated and becomes mobile.

Using the heat balance (3.7), we can determine the temperature of the top of the convecting layer of intruded melt with the overlying layer of molten country rock. In figures 3–6, we show some typical model predictions. The temperature of the new intrusion of magma is shown in solid red, the interface in green and the temperature of the roof melt layer produced by the melting of the roof material in blue. The thickness of the roof melt (black to blue lines), the cumulate layer formed at the base of the intrusion (red line) and the volume of the well-mixed crystal suspension is shown by the region between the red and black lines. The crystal mass fractions in the intrusion (red) and in the roof melt (blue) are shown on the third panel.

In figure 3, we present a reference calculation, in which we assume the intrusion of magma has a melting range 900–1100°C while the roof material is somewhat more fractionated and so has a melting range 800–1000°C. The country rock is assumed to have a temperature of 700°C. We see that the model predicts that as the intrusion of magma cools and crystallizes, there is an initial phase of cooling and crystal growth in the main melt, but with negligible cumulate formation. However, after about 100 years, the intrusion cools and becomes more crystalline, the convection decreases, and crystal settling sets in, building up the cumulate layer. As the magma cools and crystallizes, the heat released leads to melting of a part of the overlying country rock which at early times heats up until the initial crystal content of this layer is about 40%. This roof melt layer then continues to grow by partial melting of the overlying roof material, accommodating the heat released by the cooling and crystallization of the new intrusion of magma.

As the system continues to cool, the crystal content of the main body of melt progressively increases until it becomes so crystalline that it locks up above the cumulate layer. This results in a two-layer system: there is a stratified cumulate layer which has a vertical density gradient in the melt phase, owing to the progressive trapping of melt around the sedimenting crystals which form the cumulate, and there is a more uniform zone of jammed mush above.

We can assess the evolution of the density in the cumulate layer by tracking the evolution of the density of the melt as it cools and crystallizes. Assuming that the cumulate layer has a porosity or melt fraction, here taken to be 0.4, associated with the packing of the crystals, then for the calculations of figure 3, we predict that the melt becomes progressively less dense with height in the cumulate layer, according to the red reference curve shown in figure 4. This represents quite a strong density stratification of the melt owing to the large mass of crystals which form so that there is a significant decrease of the residual melt density with height in the cumulate layer.

The predictions of the model regarding (i) the balance between the depth of the cumulate and of the jammed crystal-rich mushy zone and (ii) the density stratification in the cumulate layer, depend on the cooling rate of the melt compared to the settling rate of the crystals. In turn, this depends on the difference in the melting ranges of the country rock and the intruded magma as well as the settling speed of the crystals. As the range of melting temperatures of the country rock reduces relative to that of the intruded magma, then the rate of heat transfer to the country rock increases because the roof melt layer is cooler. In order to illustrate this effect, we

Downloaded from https://royalsocietypublishing.org/ on 04 March 2022

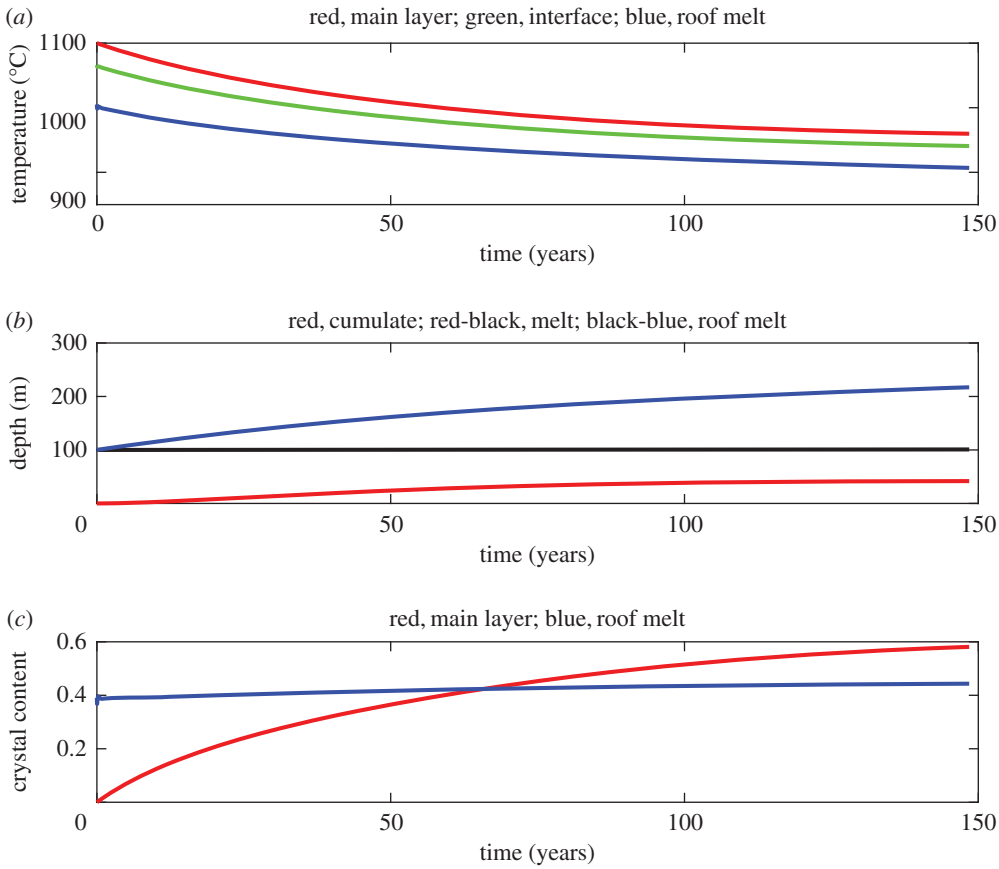

Figure 3. (*a*) Illustration of the variation with time of the melt temperature (red), the interface (green) and the roof melt (blue). Panel (*b*) shows the cumulate layer thickness (red), the roof melt thickness (black-blue) and the melt above the cumulate (red-black). Panel (*c*) shows the melt and roof melt crystal content (red and blue). Curves are shown for a 100 m deep sill with melt of viscosity 1000 Pa s and roof melt of viscosity 10 000 Pa s. The crystals are assumed to have fall speed 10^{-7} m s^{-1} in the melt, the roof melt is assumed to have a melting range 800–1000°C, while the intrusion has an assumed melting range 900–1100°C and the country rock temperature is taken to be 700°C.

present a second calculation in figure 5 corresponding to the case that the melting range of the roof material is 750–950°C, while the properties of the intruded magma remain the same as for figure 3.

In this case, the cooling process is faster, and there is less time for crystals to sediment as the intrusion cools and crystallizes. This leads to an increase in the crystal content of the convecting melt towards a jammed state (red line, panel 3) while there is much less cumulate layer formation. Meanwhile, a deeper layer of roof melt develops owing to the heat transfer from the intrusion of new magma (panel 2, blue line). In this case, the main magma intrusion evolves to form a more homogeneous crystalline layer, with only a very thin stratified cumulate zone below (black curve in figure 4).

The overall model predictions are also sensitive to a number of other factors, including the crystal size and hence fall speed. In practice, the crystal size may evolve with time, as new crystals nucleate and existing crystals grow and then sediment (cf. [38]). In order to illustrate the leading order impact of the crystal size on the evolution of the sill, in figure 6, we illustrate the evolution of the system in the case that the crystals have fall speed 2 times that shown for figure 3. According

Downloaded from https://royalsocietypublishing.org/ on 04 March 2022

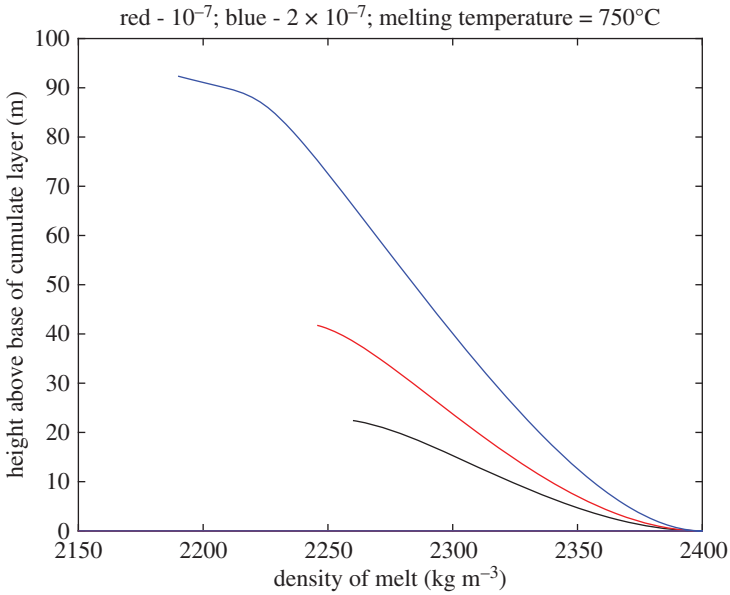

Figure 4. Model calculations of the evolution of the melt density trapped in the cumulate layer. Curves indicate the effect of the fall speed and the melting temperature of the roof melt. Red curve corresponds to a fall speed of 1×10^{-7} m s^{-1} in the main melt with melting temperature of 800°C (cf figure 3); black curve corresponds to melting temperature of 750°C and fall speed of 1×10^{-7} m s^{-1} (figure 5) and the blue curve corresponds to the case with crystal fall speed of 2×10^{-7} m s^{-1} and melting temperature of 800°C (figure 6).

to Stokes Law, the fall speed follows the relation:

$$v_s = \frac{2g\Delta\rho d^2}{9\mu}, \tag{3.15}$$

where d is the crystal size, g is the gravitational acceleration, μ the viscosity and $\Delta\rho$ denotes the density difference between the crystals and the melt μ. Therefore, an increase by a factor of 2 corresponds to an increase in crystal size by about a factor of about 1.4, as compared to the calculations in figures 3 and 5. This increase in fall speed leads to a deeper cumulate layer. Now, as the melt layer cools, there is an initial build up crystals in suspension, but this reduces the cooling rate as it increases the effective viscosity of the intrusions, and so the settling of the crystals is able to keep pace with the crystal production and eventually outrun the production, so that most crystals settle into the cumulate and trap interstitial melt. The ultimate density stratification in the cumulate layer is smaller than in the two other cases in figure 4 (blue curve) because the crystals now settle faster than the melt evolves.

The differences in the cumulate density structure and also the balance between a jammed homogeneous mush layer and the cumulate layer illustrate the sensitivity of the cooling and crystallization process: with similar parent magmas, if the settling speed of the crystals, or the degree of fractionation in the roof melt changes, all other aspects being the same quite dramatic differences may arise in the ensuing deposit.

The results of this section are important because they illustrate how the interaction of cooling and crystallization coupled with sedimentation can lead to different rates of build up of the cumulate at the base of the intrusion compared to the bulk crystal–melt layer which develops above the cumulate. The cumulate layer can become very density stratified, while the crystal-rich melt layer above remains more well-mixed through the convective stirring.

The properties and depth of cumulate which forms vary from case to case, and this implies that the composition of the remaining crystal–melt suspension will also vary. The model calculations

Downloaded from https://royalsocietypublishing.org/ on 04 March 2022

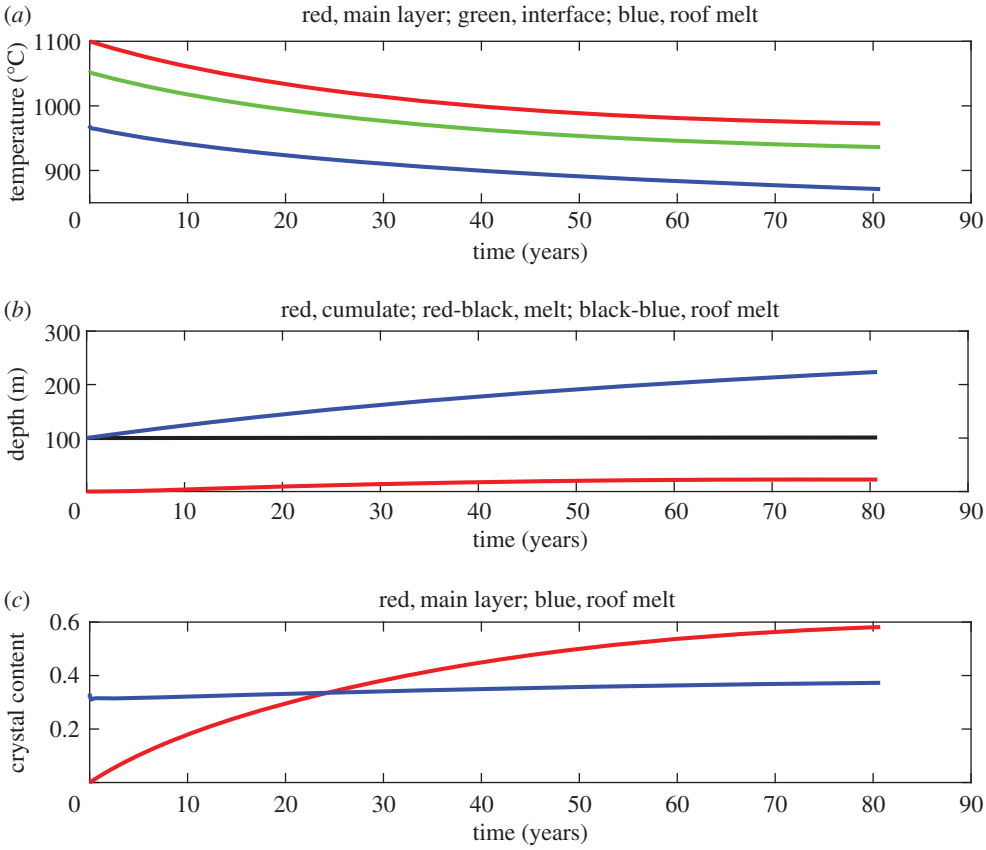

Figure 5. Illustration of the cooling of the new intrusion of melt, when the roof material has a melting range which is 150°C lower than that of the magmatic intrusion, in comparison to figure 3 where it is 100°C lower. The three panels show the temperature, the depth and the crystal content of the two melts. In the present case, the cooling of the main melt is faster than in figure 3, owing to the larger heat flux across the melt layers which drives the convection. This reduces the fraction of crystals which sediment from the main body of melt as it cools, and hence a deeper mush layer develops which eventually jams up.

illustrate, in a simplified fashion, that the crystal–melt suspension can become so crystal rich that it jams up, but that depending on the amount of cumulate formed at this point, the composition and temperature of this jammed crystal–melt mixture will also differ. This implies that the detailed fractionation history of successive intrusions of melt, even at comparable depth in the crust, may differ, leading to a diversity in the bulk composition of individual pockets of melt in the crust. However, we expect this local variability will occur in parallel with the overprint of the general fractionation trend associated with the migration of the melt upwards through the crust to progressively cooler crust. The evolution of zones of crystallized magma of different composition, illustrated by the processes herein, will tend to promote local layering and density stratification.

The present modelling points to the possible development of a heated and remobilized layer of country rock at the top of the intrusion. In the model, this roof melt layer becomes mobile once a critical fraction has melted, leading to an overlying, cooler convecting suspension of country rock. As the system evolves, this layer deepens but also cools and becomes progressively more crystalline until it has cooled sufficiently to become close-packed and jam. However, depending on the melting range of this material compared to the newly intruded magma, this molten roof layer may remain mobile for some time after the new intrusion has become so crystalline that it

Downloaded from https://royalsocietypublishing.org/ on 04 March 2022

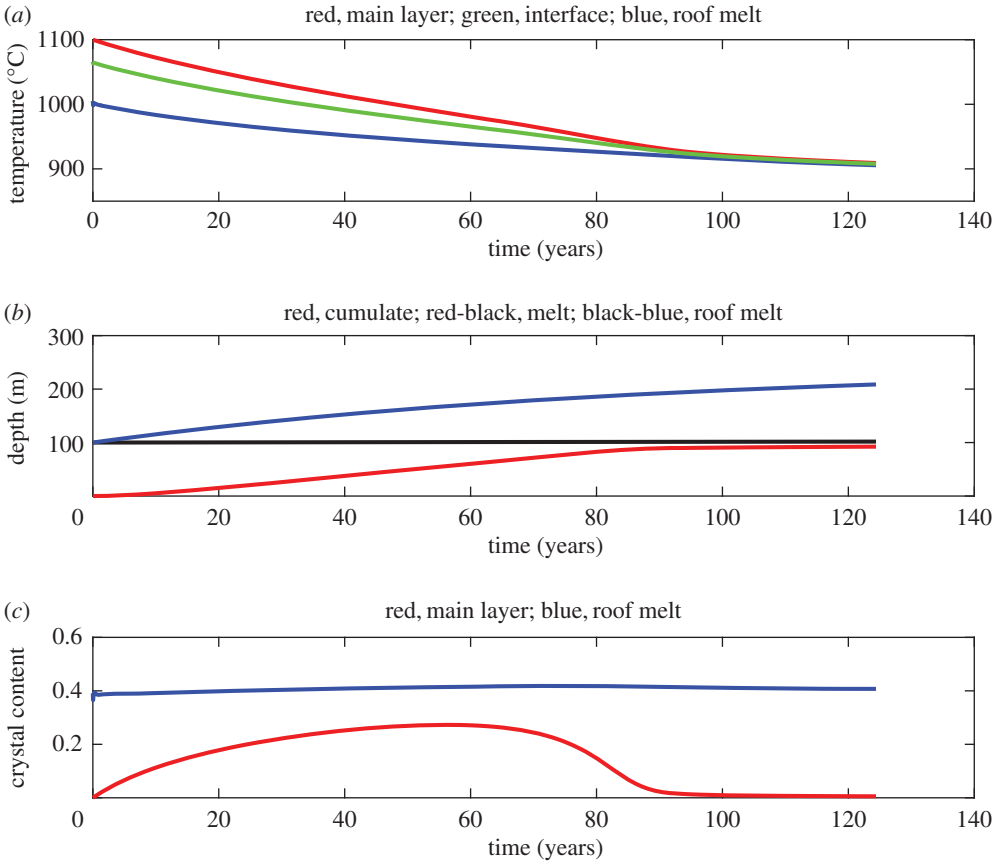

Figure 6. Illustration of the evolution of the new injection of magma lines and the roof melt produced by the heat transfer to the roof. Panel (*a*) shows the temperature, panel (*b*) the depth of the cumulate and roof melt layer and panel (*c*) illustrates the evolution of the crystal content. In this example, the crystal fall speed is 2 times the value used in figure 3, and this leads to a significant increase in the rate of accumulation of cumulate leading to the majority of the solidified sill being associated with the cumulate rather than a jammed crystal-mush zone.

jams up. As the system evolves, this may lead to reworking of the crustal material, and possible mobilization and injection to points higher in the crust.

(f) Roof cumulate

It is interesting to note that for the Icelandic melt example shown in figure 2, the main phase of cooling and plagioclase growth involves the production of buoyant crystals from a relatively dense melt. As a result, the plagioclase will tend to rise to the roof of the chamber, producing a roof cumulate, in a fashion analogous to that described above for the generation of a floor cumulate. As the melt cools and crystallizes more plagioclase, the residual melt will increase in density, leading to a stable density stratification of the melt trapped in the roof cumulate. In this case, heat transfer from the new melt to the floor of the chamber will tend to melt the floor material, assuming it is of similar origin to the new magmatic intrusion, but somewhat more evolved. If the floor melt is denser than the new intrusion, this melt layer will underlie the new magma, gradually deepening in an analogous fashion to the overlying melt layer described in the figures above. One interesting implication in this case is that if a roof cumulate layer does form, some of this layer may then be eroded and erupted during any subsequent eruption of the underlying melt (cf. [39,40]).

Downloaded from https://royalsocietypublishing.org/ on 04 March 2022

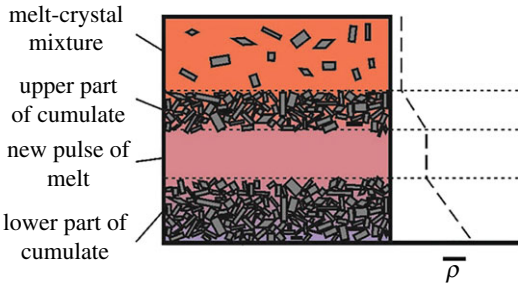

Figure 7. Illustration of the intrusion of the new melt within the density stratified cumulate layer. The chart to the right indicates the nature of the stratification in density which may arise through cooling, crystallization and sedimentation.

4. Secondary emplacement of melt

In an active vertically protracted volcanic system (e.g. [8]), one might expect that such partially solidified sills will be subject to further injection of magma of similar composition. It is therefore of interest to explore how a new intrusion might interact with a sill which has already evolved to form a bulk mushy zone from the crystalline convecting layer that overlies a stratified cumulate layer, as a result of crystal sedimentation. We focus on the injection of a magma into a relatively young system in which the melt–crystal mixture or the cumulate layer are still partially molten, and deformable, so that the buoyancy may play a role in the emplacement of the melt; in a more evolved system, it is key to remember that the solid stresses in the system likely control the migration pathways of the magma [41].

If a new batch of melt intrudes into the sill, then ensuing motion depends on the structural integrity of the interfaces between the different zones in the crust [41]. Also the motion may depend on the density of the intruding melt relative to the mobile melt–crystal mixture in the sill. As we have seen, this density varies between the cumulate layer and the overlying melt–crystal mixture.

On reaching a sill containing a mobile phase, the intruding layer of magma may rise through the cumulate, provided it can overcome any yield stress required to deform the cumulate layer [42]. The melt will then either rise through the mobile crystalline mush, if it is less dense, or it may spread out at the base of this layer. However, if the crystalline mush has become jammed, the fate of the intruding melt also depends on whether it can overcome any yield stress required to deform a channel through the layer, or if it is simpler to intrude below the crystalline layer.

The subsequent evolution of the intruding melt will now be influenced by the existing crystal laden melt layer and the stratified cumulate layer. In some cases, the interstitial melt in the cumulate layer and the overlying crystal–melt layer may be less dense than the new melt, especially if the new melt has intruded in the cumulate at the point where the bulk density of the cumulate layer matches that of the new melt (figure 7).

As the intruded melt begins to cool by contact with the colder material in the sill, it may start to convect as described above. However, as the heat from the new melt is transferred to the overlying cumulate layer, this layer will heat up and some crystals will resorb, leading to remobilization of the cumulate layer. The melt within the cumulate layer is stably stratified and this density gradient will suppress convection in the remobilized layer. However, as the intruded melt gradually cools and crystallizes, some of the crystals may sediment to the base of the layer, and the density of the remaining melt will decrease. This can lead to an unstable density stratification developing at the interface with the remobilized roof layer, and the mobilized cumulate material may gradually mix into the new intrusion.

Heat will also be transferred into the cumulate layer at the base of the new melt layer. Again this may lead to remobilization of the cumulate layer, but the stable stratification may suppress

Downloaded from https://royalsocietypublishing.org/ on 04 March 2022

Table 1. Experimental properties. Table of properties, listed by the fluid colour in each of the experiments, for the three experiments shown in figure 8. Each fluid has a specific viscosity and density as shown by the numbers in the brackets. The units are Pa s and kg[4].

experiment	yellow	red	clear
a	1.0, 1.054	0.1, 1.171	1.0, 1.060
b	1.0, 1.041	0.1, 1.093	1.0, 1.151
c	1.0, 1.045	0.1, 1.095	1.0, 1.154

significant motion unless a sufficient number of crystals are resorbed so that the relatively light melt in the cumulate layer can begin to exchange with the overlying heavier new melt.

5. Analogue experiments

The emplacement of new melt into a sill which is approaching the jammed state is a complex problem and involves the dynamics of a crystal-packed fluid in which the crystals may be in contact and can thereby support a stress. In this case, a small rearrangement or dilation of the system may lead to remobilization such as to enable a second fluid to generate a flow channel through the layer. Numerical experiments have identified some of the processes which may arise assuming a particular rheological response from the mushy zone [43]. To complement such numerical modelling, we have carried out a series of preliminary experiments to illustrate that such channelling is possible, at least in the laboratory, by filling a Perspex tank of dimension 10 cm × 10 cm × 10 cm with small acrylic particles. We mixed these with a saline and very viscous natrosol solution in order to control the liquid viscosity and density (table 1). We placed a second layer (yellow in figure 8) comprising either a viscous natrosol solution or a mixture of natrosol solution and particles. In this second solution, we used a lower salinity so that this upper layer is less dense. In each case that we used a particle-liquid layer, the layer had a particle fraction close to 0.4. We then prepared three solutions of a third viscous fluid, dyed red, each one having a different salinity, so as to have a density (i) greater than, (ii) intermediate to, and (iii) less than the bulk density of the two layers in the reservoir. The experiments enabled us to test if this fluid can indeed intrude at the different levels in the particle-laden fluid system.

In figure 8, we present some initial results which indicate that the emplacement of the new melt may be strongly influenced by the density of the particle-laden layers. In figure 8*a*, the injected fluid (red) is denser than the particle-laden layer (grey), and it intrudes along the base of the system. In the second case (figure 8*b*), the intruded red fluid is less dense than the particle-laden layer but more dense than the overlying pure fluid yellow layer; it develops a flow channel through the particle-laden zone, and then spreads out on the top of the particle-laden zone, beneath the relatively low-density fluid. In figure 8*c*, there are two layers of particle-laden fluid, a relatively dense grey layer overlain by a less dense yellow-grey layer. Above this, there is a third layer of less dense yellow fluid. The injected fluid is buoyant compared to the grey particle-laden zone at the base but dense relative to the yellow-grey particle-laden layer. We see that the injected fluid migrates to the interface and spreads out above the grey layer, but below the yellow-grey layer. In this experiment, a second subsequent injection of a fluid which was less dense than the upper yellow fluidparticle layer, led to the injected fluid breaking through the yellow-grey layer to reach the top of the tank.

The packing distribution of the particles determines the direction of least principle stress and this influences the detailed direction of the channel along which the new melt migrates, as seen comparing figure 8*b*,*c*. The images also point to the complexity of the emplacement process, and that the development of flow channels and migration of the melt can be strongly influenced by the solid stresses (cf. [41]). Indeed, the subsequent lateral intrusion of the melt into the highly viscous melt may also lead to a channeling instability, rather than a symmetric intrusion, depending on the

Downloaded from https://royalsocietypublishing.org/ on 04 March 2022

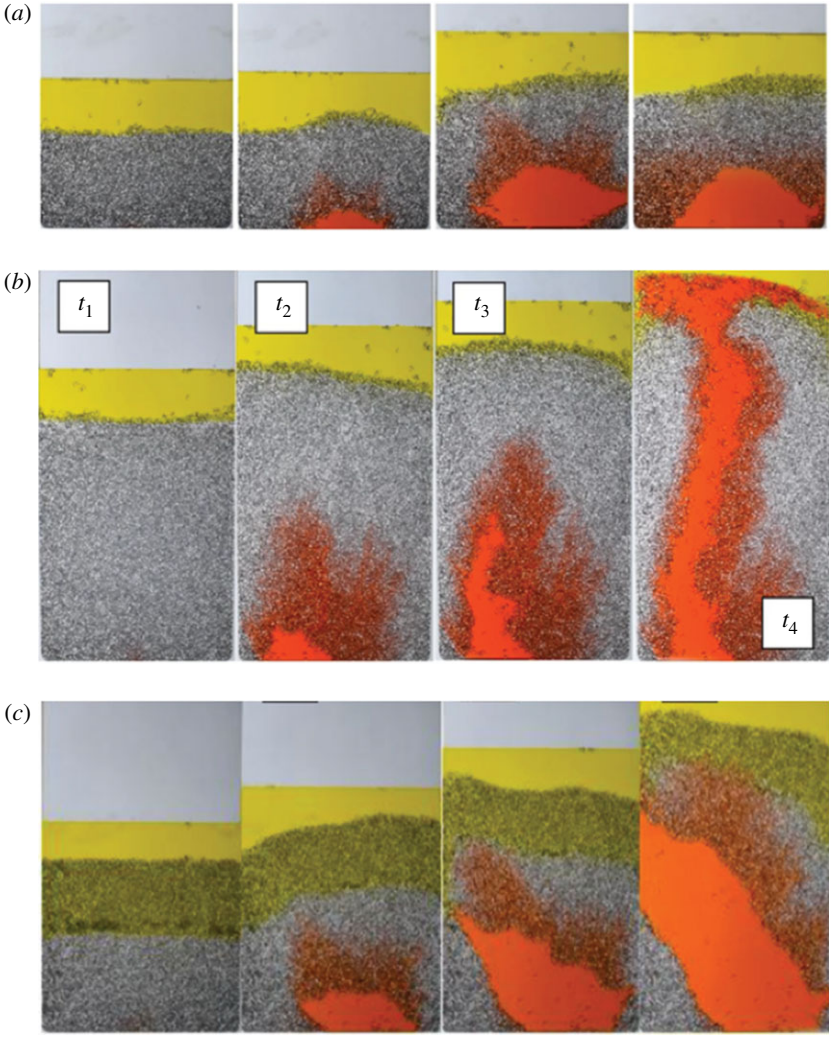

Figure 8. Preliminary experiments to explore the emplacement of a new melt into a mushy zone with density either (*a*) smaller; (*b*) more buoyant (middle row of photographs) and (*c*) stratified, with the injected liquid having an intermediate density. Properties of each experiment are shown in table 1.

depth of the layer and the magma supply rate. It will be a fascinating avenue for future research to explore these processes in more detail.

6. Conclusion and volcanological implications

Zones of volcanic activity which are underlain by thick mush sequences may have complex crustal density profiles. Where these mush sequences formed from multiple stacked sills, they will include layers that formed as cumulates at the base of the intrusions and show upwards density stratification, as well as more homogeneous zones that formed from the jammed-up intrusion interiors. The controls on the division between cumulate and mush zones is governed by a competition between the cooling and crystal production time compared to the crystal settling. Interactions between successive intrusions can therefore lead to alternation in density and composition of individual layers. It has been proposed that convection leads to homogeneous crystal mushes, such as observed with crystal-rich dacites and large silicic plutons [44]. This is in accord with the present model in which the crystal mush becomes jammed by the growth

Downloaded from https://royalsocietypublishing.org/ on 04 March 2022

of crystals in suspension (e.g. Figures 3 and 5), especially when the crystal sedimentation time exceeds the cooling and crystallization time so that the crystals do not sediment to the base of the system. By contrast, with faster crystal fall speeds, the main part of the intrusion evolves into the stratified cumulate zone.

The model suggests that in long-lived, vertically extensive magmatic systems (e.g. [8]) the sub-volcanic mush is likely to be heterogeneous with respect to its density and composition on short length-scales. This has important implications for the dynamics of such systems, impacting the depths at which melts are intruded and the ability for magmas to ascend through the crust (e.g. [41,45]). As this new paradigm of trans-crustal magmatic systems is developed, such heterogeneity may have an important influence on the details of the magma evolution. Subtle changes in the cooling rate, the thickness of a sill or the degree of fractionation of the magma can lead to changes between a jammed homogeneous mush and a density stratified cumulate forming. On larger vertical length-scales, mush systems will become more systematically stratified, with the most evolved and lowest density material able to ascend to the highest crustal levels [10]. However, the parent melts from which specific cumulate zones are generated may become spatially dislocated from the cumulates as a result of the intrusion of new melt if this intrusion has a density which intersects the density gradient which may naturally develop within a cumulate.

More tentatively, field observations of intrusive complexes, such as Bushveld (South Africa) and Rum (Scotland), do preserve evidence of vertical gradients in magma composition and mush density. These include both graded and homogeneous layers, which may be represented by the cumulate and jammed sill interior zones in our models, respectively [46–48] and recent studies have suggested that some layering in these intrusions formed as sills intruded into pre-existing, partially solidified mush [49,50]. Although there are certainly other complex physico-chemical processes in operation [51], the fluid mechanical phenomena discussed in this contribution are likely to have played a role in the genesis of some of the layering and structure of such formations.

We also note that a number of works have focused on the possible role of compaction in generating large bodies of melt from crystalline mush zones (e.g. [52,53]). The present modelling suggests that with sufficiently rapid crystal settling, the melt within a cumulate layer will become density stratified. If this is the case, any compaction driven separation of the melt will need to overcome the density stratification, and may lead to a density stratified melt zone. The formation of channels in a crystal layer to enhance the melt–crystal segregation may be impacted by such stratification, and may lead to differences in the efficacy of melt-segregation from cumulate and jammed crystal-mush layers, in which the melt is likely to be more homogeneous. It would be of interest to explore this in future work.

Data accessibility. This article has no additional data.

Competing interests. We declare we have no competing interests.

Funding. We received no funding for this study.

Acknowledgements. M.J.S. acknowledges support from a Junior Research Fellowship at Christ's College, Cambridge.

References

1. Hildreth W, Moorbath S. 1988 Crustal contributions to arc magmatism in the Andes of central Chile. *Contrib. Mineral. Petrol.* **98**, 455–489. (doi:10.1007/BF00372365)
2. Rudnick RL, Fountain DM. 1995 Nature and composition of the continental crust: a lower crustal perspective. *Rev. Geophys.* **33**, 267–309. (doi:10.1029/95RG01302)
3. Annen C, Blundy JD, Sparks RSJ. 2005 The genesis of intermediate and silicic magmas in deep crustal hot zones. *J. Petrol.* **47**, 505–539. (doi:10.1093/petrology/egi084)
4. Annen C, Blundy JD, Leuthold J, Sparks RSJ. 2015 Construction and evolution of igneous bodies: towards an integrated perspective of crustal magmatism. *Lithos* **230**, 206–221. (doi:10.1016/j.lithos.2015.05.008)
5. Marsh B. 2004 A magmatic mush column rosetta stone: the McMurdo Dry Valleys of Antarctica. *Eos, Trans. Amer. Geophys. Union* **85**, 497–502. (doi:10.1029/2004EO470001)

Downloaded from https://royalsocietypublishing.org/ on 04 March 2022

6. Christopher TE, Blundy J, Cashman K, Cole P, Edmonds M, Smith PJ, Sparks RSJ, Stinton A. 2015 Crustal-scale degassing due to magma system destabilization and magma-gas decoupling at Soufrière Hills Volcano, Montserrat. *Geochem. Geophys. Geosyst.* **16**, 2797–2811. (doi:10.1002/2015GC005791)
7. Bachmann O, Huber C. 2016 Silicic magma reservoirs in the Earth's crust. *Am. Mineral.* **101**, 2377–2404. (doi:10.2138/am-2016-5675)
8. Cashman *et al.* 2017.
9. Sparks RSJ, Cashman KV. 2017 Dynamic magma systems: implications for forecasting volcanic activity. *Elements* **13**, 35–40. (doi:10.2113/gselements.13.1.35)
10. Jagoutz O, Schmidt MW. 2012 The formation and bulk composition of modern juvenile continental crust: the Kohistan arc. *Chem. Geol.* **298**, 79–96. (doi:10.1016/j.chemgeo.2011.10.022)
11. Lipman PW, Bachmann O. 2015 Ignimbrites to batholiths: integrating perspectives from geological, geophysical, and geochronological data. *Geosphere* **11**, 705–743. (doi:10.1130/GES01091.1)
12. Huppert HE, Sparks RSJ, Turner JS. 1982 Effects of vol-atiles on mixing in calc-alkaline magma systems. *Nature* **297**, 554–560.
13. Huppert HE, Sparks RSJ. 1988 The generation of granitic magma by intrusion of basalt in the continental crust. *J Petrol.* **29**, 599–624.
14. Sparks RSJ, Meyer P, Sigurdsson H. 1980 Density variation amongst mid ocean ridge basalts, implications for magma mixing and the scarcity of primitive lavas. *Earth Planet Sci. Lett.* **46**, 419–430.
15. Thomas N, Tait S, Koyaguchi T. 1993 Mixing of stratified liquids by the motion of gas bubbles: application to magma mixing. *Earth Planet. Sci. Lett.* **115**, 161–175.
16. Phillips JC, Woods AW. 2002 Suppression of large scale magma mixing by melt-volatile separation. *Earth Planet. Sci. Lett.* **204**, 47–60. (doi:10.1016/S0012-821X(02)00978-0)
17. Fisk MR, Schilling JG, Sigurdsson H. 1980 An experimental investigation of Iceland and Reykjanes Ridge tholeiites: I. Phase relations. *Contrib. Mineral. Petrol.* **74**, 361–374. (doi:10.1007/BF00518117)
18. Grove TL, Kinzler RJ, Bryan WB. 1992 Fractionation of mid-ocean ridge basalt (MORB). *Mantle Flow Melt Gen. Mid-Ocean Ridges* **71**, 281–310.
19. Barclay J, Rutherford MJ, Carroll MR, Murphy MD, Devine JD, Gardner J, Sparks RSJ. 1998 Experimental phase equilibria constraints on pre-eruptive storage conditions of the Soufrière Hills magma. *Geophys. Res. Lett.* **25**, 3437–3440. (doi:10.1029/98GL00856)
20. Wilke S, Holtz F, Neave DA, Almeev R. 2017 The effect of anorthite content and water on Quartz–Feldspar cotectic compositions in the rhyolitic system and implications for geobarometry. *J. Petrol.* **58**, 789–818. (doi:10.1093/petrology/egx034)
21. Danyushevsky LV, Plechov P. 2011 Petrolog3: Integrated software for modeling crystallization processes. *Geochem. Geophys. Geosyst.***12**, GC003516. (doi:10.1029/2011GC003516)
22. Gualda GA, Ghiorso MS, Lemons RV, Carley TL. 2012 Rhyolite-MELTS: a modified calibration of MELTS optimized for silica-rich, fluid-bearing magmatic systems. *J. Petrol.* **53**, 875–890. (doi:10.1093/petrology/egr080)
23. Lange RA. 1997 A revised model for the density and thermal expansivity of K_2O-Na_2O-CaO-MgO-Al_2O_3-SiO_2 liquids from 700 to 1900 K: extension to crustal magmatic temperatures. *Contrib. Mineral. Petrol.* **130**, 1–11.
24. Ochs FA, Lange RA. 1999 The density of hydrous magmatic liquids. *Science* **283**, 1314–1317. (doi:10.1126/science.283.5406.1314)
25. Smyth JR, McCormick TC. 1995 Crystallographic data for minerals. *Min. Phys. Crystallogr. A Handb. Phys. Constants* **2**, 1–17. (doi:10.1029/RF002p0001)
26. Plail M, Barclay J, Humphreys MC, Edmonds M, Herd RA, Christopher TE. 2014 Characterization of mafic enclaves in the erupted products of Soufrière Hills Volcano, Montserrat, 2009 to 2010. *Geol. Soc. Lond. Mem.* **39**, 343–360. (doi:10.1144/M39.18)
27. Devine JD, Rutherford MJ, Norton GE, Young SR. 2003 Magma storage region processes inferred from geochemistry of Fe–Ti oxides in andesitic magma, Soufriere Hills Volcano, Montserrat, WI. *J. Petrol.* **44**, 1375–1400. (doi:10.1093/petrology/44.8.1375)
28. Edmonds M *et al.* 2014 Pre-eruptive vapour and its role in controlling eruption style and longevity at Soufrière Hills Volcano. *Geol. Soc. Lond. Mem.* **39**, 291–315. (doi:10.1144/M39.16)

Downloaded from https://royalsocietypublishing.org/ on 04 March 2022

29. Gleeson ML, Stock MJ, Pyle DM, Mather TA, Hutchison W, Yirgu G, Wade J. 2017 Constraining magma storage conditions at a restless volcano in the Main Ethiopian Rift using phase equilibria models. *J. Volcanol. Geotherm. Res.* **337**, 44–61. (doi:10.1016/j.jvolgeores.2017.02.026)
30. Shorttle O, Maclennan J. 2011 Compositional trends of Icelandic basalts: Implications for short–length scale lithological heterogeneity in mantle plumes. *Geochem. Geophys. Geosyst.* **12**, GC003748. (doi:10.1029/2011GC003748)
31. Winpenny B, Maclennan J. 2011 A partial record of mixing of mantle melts preserved in Icelandic phenocrysts. *J. Petrol.* **52**, 1791–1812. (doi:10.1093/petrology/egr031)
32. Neave DA, Maclennan J, Thordarson, T, Hartley ME. 2015 The evolution and storage of primitive melts in the Eastern Volcanic Zone of Iceland: the 10 ka Grímsvötn tephra series (ie the Saksunarvatn ash). *Contrib. Mineral. Petrol.* **170**, 21. (doi:10.1007/s00410-015-1170-3)
33. Hartley, M, Maclennan J. 2018 Magmatic densities control erupted volumes in Icelandic volcanic systems. *Front. Earth Sci.* **6**, 29. (doi:10.3389/feart.2018.00029)
34. Martin D, Nokes R. 1988 Crystal settling in a vigorously converting magma chamber. *Nature* **332**, 534–536. (doi:10.1038/332534a0)
35. Turner JS. 1979 *Buoyancy effects fluids*. Cambridge, UK: Cambridge University Press.
36. Davaille A, Jaupart C. 1993 Transient high Rayleigh number convection with large viscosity contrasts. *J. Fluid Mech.* **253**, 141–166. (doi:10.1017/S0022112093001740)
37. Roscoe R. 1952 The viscosity of suspensions of rigid spheres. *Br. J. Appl. Phys.* **3**, 267–269. (doi:10.1088/0508-3443/3/8/306)
38. Jarvis R, Woods AW. 1994 The nucleation, growth and settling of crystals from a turbulently convecting melt. *J. Fluid Mech.* **273**, 83–107. (doi:10.1017/S0022112094001850)
39. Deering CD, Bachmann O, Vogel TA. 2011 The Ammonia Tanks Tuff: erupting a melt-rich rhyolite cap and its remobilized crystal cumulate. *Earth Planet. Sci. Lett.* **310**, 518–525. (doi:10.1016/j.epsl.2011.08.032)
40. Neave DA, Maclennan J, Hartley, ME, Edmonds M. 2014 Thorvaldur thordarson crystal storage and transfer in basaltic systems: the Skuggafjöll Eruption, Iceland. *J. Petrology* **55**, 2311–2346. (doi:10.1093/petrology/egu058)
41. Menand T. 2011 Physical controls and depth of emplacement of igneous bodies: a review. *Tectonophysics* **500**, 11–19. (doi:10.1016/j.tecto.2009.10.016)
42. Bergantz GW, Schleicher JM, Burgisser A. 2017 On the kinematics and dynamics of crystal-rich systems. *J. Geophys. Res. Solid Earth* **122**, 6131–6159. (doi:10.1002/2017JB014218)
43. Bergantz GW, Schleicher JM, Burgisser A. 2015 Open-system dynamics and mixing in magma mushes. *Nat. Geosci.* **8**, 793–796. (doi:10.1038/ngeo2534)
44. Huber C, Bachmann O, Manga M. 2009 Homogenization processes in silicic magma chambers by stirring and mushification (latent heat buffering). *Earth Planet. Sci. Lett.* **283**, 38–47. (doi:10.1016/j.epsl.2009.03.029)
45. Burgisser, A, Bergantz GW. 2011 A rapid mechanism to remobilize and homogenize highly crystalline magma bodies. *Nature* **471**, 212–215. (doi:10.1038/nature09799)
46. Ashwal LD, Webb SJ, Knoper MW. 2005 Magmatic stratigraphy in the Bushveld Northern Lobe: continuous geophysical and mineralogical data from the 2950 m Bellevue drillcore. *S. Afr. J. Geol.* **108**, 199–232. (doi:10.2113/108.2.199)
47. Holness MB, Winpenny BEN. 2008 The Unit 12 allivalite, Eastern Layered Intrusion, Isle of Rum: a textural and geochemical study of an open-system magma chamber. *Geol. Mag.* **146**, 437–450. (doi:10.1017/S0016756808005797)
48. Hayes B, Ashwal LD, Webb SJ, Bybee GM. 2017 Large-scale magmatic layering in the Main Zone of the Bushveld Complex and episodic downward magma infiltration. *Contrib. Mineral. Petrol.* **172**, 13. (doi:10.1007/s00410-017-1334-4)
49. Holness MB. 2005 Spatial constraints on magma chamber replenishment events from textural observations of cumulates: the Rum Layered Intrusion, Scotland. *J. Petrol.* **46**, 1585–1601. (doi:10.1093/petrology/egi027)
50. Mungall JE, Kamo SL, McQuade S. 2016 U–Pb geochronology documents out-ofsequence emplacement of ultramafic layers in the Bushveld Igneous Complex of South Africa. *Nat. Commun.* **7**, 13385. (doi:10.1038/ncomms13385)

51. Namur O *et al.* 2015 Igneous layering in basaltic magma chambers. In *Layered intrusions* (eds B Charlier, O Namur, R Latypov, C Tegner), pp. 75–152. Dordrecht, The Netherlands: Springer.
52. Solano JMS, Jackson MD, Sparks RSJ, Blundy JD, Annen C. 2012 Melt segregation in deep crustal hot zones: a mechanism for chemical differentiation, crustal assimilation and the formation of evolved magmas. *J. Petrol.* **53**, 1999–2026. (doi:10.1093/petrology/egs041)
53. Bachmann O, Bergantz GW. 2004 On the origin of crystal-poor rhyolites: extracted from batholithic crystal mushes. *J. Petrol.* **45**, 1565–1582. (doi:10.1093/petrology/egh019)

Downloaded from https://royalsocietypublishing.org/ on 04 March 2022